Published in final edited form as:

Circ Res. 2018 June 08; 122(12): 1675–1688. doi:10.1161/CIRCRESAHA.117.312513.

Atlas of the immune cell repertoire in mouse atherosclerosis defined by single-cell RNA-sequencing and mass cytometry

Holger Winkels[1,*], **Erik Ehinger**[1,*], **Melanie Vassallo**[1], **Konrad Buscher**[1], **Huy Dinh**[1], **Kouji Kobiyama**[1], **Anouk A.J. Hamers**[1], **Clément Cochain**[2], **Ehsan Vafadarnejad**[3], **Antoine-Emmanuel Saliba**[3], **Alma Zernecke**[2], **Akula Bala Pramod**[1], **Amlan Ghosh**[1], **Nathaly Anto Michel**[4], **Natalie Hoppe**[4], **Ingo Hilgendorf**[4], **Andreas Zirlik**[4], **Catherine C. Hedrick**[1], **Klaus Ley**[1,†], and **Dennis Wolf**[1,4,†]

[1]La Jolla Institute for Allergy and Immunology, Division of Inflammation Biology, La Jolla, CA, USA

[2]Institute of Experimental Biomedicine, University Hospital Würzburg, Würzburg, Germany

[3]Helmholtz Institute for RNA-based Infection Research, Würzburg, Germany

[4]Department of Cardiology and Angiology I, University Heart Center Freiburg, and the Faculty of Medicine, University of Freiburg, Freiburg, Germany

Abstract

Rationale—Atherosclerosis is a chronic inflammatory disease that is driven by the interplay of pro- and anti-inflammatory leukocytes in the aorta. Yet, the phenotypic and transcriptional diversity of aortic leukocytes is only poorly understood.

Objective—We characterized leukocytes from healthy and atherosclerotic mouse aortas in-depth by single cell RNA-sequencing (scRNAseq) and mass cytometry (CyTOF) to define an atlas of the immune cell landscape in atherosclerosis.

Methods and Results—Employing scRNAseq of aortic leukocytes from chow (CD) and western diet (WD) fed *Apoe*$^{-/-}$ and *Ldlr*$^{-/-}$ mice, we detected 11 principal leukocyte clusters with distinct phenotypical and spatial characteristics, while the cellular repertoire in healthy aortas was less diverse. Gene set enrichment analysis on a single cell level established that multiple pathways, such as for lipid metabolism, proliferation, and cytokine secretion, were confined to particular leukocyte clusters. Leukocyte populations were differentially regulated in atherosclerotic *Apoe*$^{-/-}$ and *Ldlr*$^{-/-}$ mice. We confirmed the phenotypic diversity of these clusters with a novel CyTOF 35-marker panel with metal-labelled antibodies and conventional flow cytometry. Cell populations retrieved by these protein-based approaches were highly correlated to transcriptionally defined clusters. In an integrated screening strategy of scRNAseq, CyTOF, and FACS, we detected three principal B-cell subsets with alterations in surface markers, functional pathways, and *in vitro* cytokine secretion. Finally, we used leukocyte cluster gene signatures to enumerate leukocyte

Correspondence to: Dennis Wolf, MD, La Jolla Institute for Allergy and Immunology, 9420 Athena Circle, 92037, La Jolla, CA, USA, dwolf@lji.org, Tel: (858) 752-6655.

*H.W. and E.E. contributed equally.

†K.L and D.W. share senior authorship

Disclosures

All authors have declared that no conflict of interest exists.

frequencies in 126 human plaques by a genetic deconvolution strategy. This approach revealed that human carotid plaques and microdissected mouse plaques were mostly populated by macrophages, T-cells, and monocytes. In addition, the frequency of genetically defined leukocyte populations in carotid plaques predicted cardiovascular events in patients.

Conclusion—The definition of leukocyte diversity by high-dimensional analyses enables a fine-grained analysis of aortic leukocyte subsets, reveals new immunological mechanisms and cell-type specific pathways, and establishes a functional relevance for lesional leukocytes in human atherosclerosis.

Subject codes

Vascular Biology; Atherosclerosis; Inflammation

Keywords

leukocytes; macrophages; lymphocytes; single cell RNA-sequencing; mass cytometry; flow cytometry

Introduction

Atherosclerosis and its complications, myocardial infarction and stroke, represent the leading cause of mortality world-wide[1]. Atherosclerosis is characterized by the build-up of leukocyte-rich plaques in the intimal layer of large and medium-sized arteries. Experimental laboratory research has established that atherosclerosis is an inflammatory disease of the arterial wall, initiated and maintained by the influx, proliferation, and activation of immune cells[2]. Atherogenesis is shaped by the interplay of pro- and anti-atherogenic leukocytes both within the atherosclerotic aorta and systemically[3]. The principal hematopoietic lineages found in the atherosclerotic aorta of rodents were discovered by fluorescence-based flow cytometry in 2006[4]. With the development and validation of state-of-the-art, high-dimensional parameter analysis tools – such as mass cytometry and single cell transcriptomics[5, 6] – it is now increasingly appreciated that flow cytometry is unable to fully elucidate the actual complexity of immune cell subsets. Specialized leukocyte subsets may be distinct in function although they express the same principal lineage markers[7]. In atherosclerosis, the diversity of plaque leukocytes on a single cell level and their relative frequencies are incompletely defined. Here, we applied two novel approaches – scRNAseq and CyTOF – to precisely define leukocytes in mouse and human atherosclerosis. Our results indicate an unexpected heterogeneity: We found that aortic leukocytes have a complexity similar to that of leukocytes in lymphoid organs and identified several novel leukocyte sub-populations that are differentially regulated in disease and may predict cardiovascular events in humans.

Material and Methods

A Material and Methods section is available in the online-only supplement.

Results

The single cell transcriptome identifies 11 distinct leukocyte populations in the atherosclerotic aorta

Flow cytometry of aortic leukocytes has emerged as accepted technique in atherosclerosis reseach[4, 8]. However, the phenotypes and transcriptomes of aortic leukocytes have remained on an inchoate level. Here, we hypothesized that a screening approach by single cell transcriptomics (scRNAseq) to detect clusters of cells that share phenotypic and transcriptional similarity may be superior to conventional, pre-selected marker driven flow cytometry. Therefore, viable aortic CD45$^+$ leukocytes from chow diet (CD) or western diet (WD)-fed female *Apoe*$^{-/-}$ mice were flow sorted (Fig. 1a, Online-Fig.Ia) from the thoracic and abdominal aorta. We confirmed larger and more complicated atherosclerotic lesions in cross-sections of the aorta from WD- compared to CD-fed *Apoe*$^{-/-}$ mice (Fig.1b, Online-Fig.Ib). After sequencing, we detected transcripts from 1,138 different genes with >257,000 sequencing reads per cell in the merged dataset of aortas from CD and WD-fed mice (Online-Fig.II). To group cells with similar gene expression, we applied an unsupervised cluster detection algorithm (SEURAT), and detected 11 leukocyte clusters that were mostly distinguishable by hematopoietic lineage-defining genes, such as *Itgam*, *Cd19*, and *Cd3e* (Fig.1b,c, Online-Fig.III). We found that *Cd3e*$^+$ T-cells accounted for 49%, *Cd19*$^+$ B-cells for 27%, *Itgam*$^+$ (CD11b$^+$) myeloid cells for 22%, and *Klrb1c*$^+$ Nk-cells for 2% of leukocytes. To validate the exact leukocyte cluster identities in an unsupervised approach, we compared their transcriptomes to published transcriptomes from mouse peripheral blood mononuclear cells (PBMCs)[9]. Based on the genetic overlap between found clusters and reference genomes (Online-Fig.IV), we found 5x T-cell (CD4$^+$/CD8$^+$ T-cells), 2x B-cell, 1x macrophage, 2x monocyte, and 1x Nk-cell population. This lineage commitment was also reflected by differentially expressed (DE) genes for each of the clusters against all remaining (Fig.1e, Online-TableI), including *Cd79b*, *Ebf1*, *Mzb1* (B-cells), *Cd4*, *Cd8* (T-cells), *Klrb1a* (Nk-cells), or *Csf1r*, *Adgre1*, *Cd68* (macrophages). In addition, we applied conventional multi-color flow cytometry with a 14-marker panel (Online-TableII) on the input cells for scRNAseq and applied an accepted gating strategy (Online-Fig.Va,b). We validate that the frequencies of B-, myeloid, and Nk-cells were comparable to these defined by protein-based flow cytometry with the exception of some T-cell subsets that remained undefined by flow cytometry (Online-Fig.Va,c).

Because we observed a significant overlap in global DE-genes between the two B-cell-, and between the myeloid cell clusters, we next identified DE-genes within the principal leukocyte lineages. Between the two monocyte subsets (*Itgam*$^+$ *Adgre1*^{low}) we found an enhanced expression of the inflammatory genes *S100a8*, *S100a9*, *Cxcl2*, *Ccl2*, *Ccl3*, *F10*, *Tnf*, and *Ly6c2* in cluster 9, suggestive of Ly6C$^+$ inflammatory monocytes. T cell clusters mainly varied in the expression of the transcription factors *Rorc*, coding for the T_H17-defining transcription factor RORγT (cluster 5), for the T_H2-defining transcription factor *Gata3* and for the respective cytokines IL-4 and IL-13 (cluster 6). In cluster 3, we did not detect differentially expressed transcription factors, but a predominant expression of the genes *Sell* and *Il7r* (coding for memory markers CD62L and IL-7R), suggestive of a population of memory T-cells. One T-cell cluster contained *Cd8a*$^+$ cytotoxic T-cells (cluster

10), while T-cell cluster 1 contained transcripts coding for both CD8 and CD4, therefore likely reflecting a mixed cell population. B-cell clusters 1 and 2 did not differ relevantly in known B-cell lineage markers. Collectively, these data establish the proportions and selective gene expression patterns of aortic leukocytes.

Spatial and numeric differences in the aortic immune cell repertoire in atherosclerosis

Because the detected leukocyte clusters in whole atherosclerotic aortas likely contained tissue-resident vascular leukocytes, we applied scRNAseq on aortic leukocytes from 8-week old, healthy *Apoe*$^{-/-}$ mice and observed only 5 principal leukocyte clusters (Online-Fig.VI): 2x macrophage, 1x T-cell, 1x B-cell, and 1x monocyte cluster, proposing that leukocyte heterogeneity is lower in healthy aortas. For instance, we observed only one T-cell cluster that was transcriptionally similar to the memory T-cell containing cluster in atherosclerotic mice. Both macrophage clusters expressed *Cx3cr1*, the marker for tissue resident, self-renewing arterial macrophages, but differed in the expression of *Lyve1* (tissue-resident) and *Ly6c* (recruited): *Lyve1*^{low}*Ly6c1*^{neg} (cluster 4) vs. *Lyve1*^{neg}*Ly6c1*$^{+}$ (cluster 5). Monocytes showed an overlapping gene signature with published genomes of Ly6c^{+} inflammatory monocytes. Next, we asked how the relative frequencies of leukocyte subsets change in *Apoe*$^{-/-}$ mice fed with a WD compared to a CD for 12 weeks. Because input cell numbers differed by more than 2-fold in WD, we followed an iterative approach by down-sampling both input cell populations repetitively to increase the statistical robustness. Among a total of 11 leukocyte clusters in the CD and WD groups, we observed 4 populations that increased, while 5 populations decreased (Fig.2b). For instance, the macrophage-containing cluster increased by 110%, while the T_H2-cell containing cluster retracted by 60%.

Because leukocyte clusters in our approach reflect a mix of adventitial, lesional, and leukocytes in the media of the artery, we addressed the spatial distribution of these cell populations. Since scRNAseq and flow cytometry require a relatively large input of cell numbers and because the digestion of aortas may affect the survival of particular leukocyte clusters, we applied a genetic deconvolution (GD) method[10], which allows to robustly calculate the relative frequency of specific cellular leukocyte signatures in bulk mRNA expression data sets also containing mRNA from non-CD45^{+} cells. Based on the expression of cluster DE-genes of scRNAseq-defined aortic leukocyte clusters, we constructed gene signatures, which were highly specific for the input cluster gene-expression data sets (Online-Fig.VIIb) and which detected frequencies of principal hematopoietic lineages in bulk transcriptomes of blood, spleen, and lymph nodes in the expected and flow-cytometry-validated range (Online-Fig.VIIc,d). We applied these aortic signatures to a GD within whole tissue mRNA expression data sets of whole aortas from *Apoe*$^{-/-}$ mice and found a cellular composition predominated by myeloid cells, including macrophages and monocytes (Online-Fig.VIId), indicating these lineages are under-represented in digestion-based scRNAseq and flow cytometry. On the level of major lineages, this composition was also confirmed in a GD of published mouse PBMC signature[18]. Next, we applied the aortic leukocyte signatures to a GD within bulk mRNA expression of laser-microdissected tissue specimen from atherosclerotic lesions, the aortic media, adventitia absent from tertiary lymphoid organs (ATLO), and adventitia with ATLOs in aged, WD-fed *Apoe*$^{-/-}$ mice (>60 weeks)[11]. We found that atherosclerotic lesions were predominantly populated by

macrophages, monocytes, and T-cells, while ATLO-rich adventitial tissue was dominated by B-cells. The overall leukocyte signal was relatively higher in ATLO-rich adventitial tissue, rendering this compartment as one of the major immune cell reservoirs in late atherosclerosis. Finally, we asked to which extent the two commonly used atherosclerosis models, *Apoe*- and *Ldlr*-deficiency, impact on the cellular composition in aortas. Therefore, we directly compared the frequency of principal leukocyte lineages by scRNAseq from CD- and WD-fed $Ldlr^{-/-}$ mice (Fig.2d, Online-Table3). The content of B-cells (higher in $Apoe^{-/-}$ mice) and macrophages (higher in $Ldlr^{-/-}$ mice) differed in aortas from both genotypes after a WD, while on a CD the cellular composition was comparable in both genotypes and relatively dominated by T-cells. These data establish the spatial and temporal dynamics of leukocyte composition of atherosclerotic aortas.

Cell-type specific genetic pathways in aortic leukocytes

In contrast to bulk tissue gene expression, scRNAseq enables a selective analysis of gene expression on a single cell level. To identify cell- or lineage-specific gene expression, we tested the enrichment of curated pathways on a single cell level by calculating gene expression scores (Fig.3a-c, Online-Fig.VIII). Interestingly, most of the tested pathways overlaid on specific cell-types: Myeloid-cells (macrophages and monocytes) over-expressed genes implicated in lipid- and cholesterol metabolism (GSEA-M5892, including *Abca1*, *Abcg1*, *Ldlr*), genes associated with apoptosis (GSEA-M8492, including caspases and TNF-signaling), and genes required for the activation of the inflammasome (GSEA-M1063, including *Nlrp3*, *P2rx7*, *Txn*). Genes correlating with acute myocardial infarction (GSEA-M15394, including genes coding for collagens, tissue factor, and fibrinogen) were enriched in Ly-6C$^+$ monocytes. On the contrary, the T_H2 cell containing cluster was enriched for genes implicated in cytokine-secretion (GSEA-M6910), proliferation, and chemokine secretion (GSEA-M4844). In addition, we performed Ingenuity Pathway Analysis (IPA) by testing cluster genes increased and decreased in WD-fed compared to CD-fed $Apoe^{-/-}$ mice (Online-TableIV). This strategy allowed us to establish a map of disease-related genetic programs in aortic leukocytes: For instance, macrophages up-regulated signaling events associated with iNOS, the main transcription factor for the pro-inflammatory M1 phenotype[12], and the group of the pro-atherogenic IRF transcription factors[13]. However, the observed higher expression of iNOS did not induce a M1-like transcriptome in macrophages in WD-fed mice (Online-Fig.VIII), indicating that the M1/M2-classification may not accurately reflect an *in vivo* phenotype. In contrast, TGF-β, a driver of plaque stabilization[14], decreased in plaque macrophages from WD-fed animals. In addition, we observed a decrease of anti-inflammatory IL-10 signaling events in the Ly-6C$^-$ monocyte-containing cluster. In accord with the concept of enhanced pro-inflammatory pathways in atherosclerosis, CD4$^+$/CD8$^+$ T-cells, memory T-cells, and CD8$^+$ T-cells switched their transcriptional profile from a recruitment-phenotype in CD-fed mice (homing receptors and genes required for cellular motility) to a more pro-inflammatory phenotype, including an up-regulation of IFN-γ signaling in WD-fed mice. Furthermore, some pathways were regulated diversely in clusters (Online-TableV): Hypoxia-induced pathways were downregulated in macrophages under a WD, but up-regulated in T_H2-cells, while TGF-β was down-regulated in macrophages, and up-regulated in Ly-6C$^+$ monocytes. These data emphasize the necessity to test gene expression on a single cell level for an unbiased approach and suggest

scRNAseq as powerful tool to combine cell cluster detection and lineage-specific gene expression at the same time.

Mass cytometry (CyTOF) confirms the phenotypical heterogeneity of aortic leukocytes

Because leukocyte phenotyping is traditionally based on the expression of surface protein markers, we applied mass cytometry (CyTOF) and tested a panel of 35 metal-labelled pan-leukocyte antibodies (Fig.4a, Online-TableVI). To optimize the detection of the small number of aortic leukocytes, we spiked cell suspensions with splenocytes from age-matched CD45.1 *Apoe*$^{-/-}$ mice that were later excluded from analysis (Fig.4b,c). To establish cell clustering and lineage detection by protein markers, aortic leukocytes from *Apoe*$^{-/-}$ mice fed a CD or WD for 12 weeks were acquired on CyTOF and separated into cell clusters by a CyTOF-adapted dimensionality reduction and cluster detection algorithm (PhenoGraph, Fig. 4d). Of 28 clusters from aortas from CD and WD-fed mice, we found 23 unique cell clusters above the selected frequency threshold of 1% (Fig.4d, Online-TableVII). This heterogeneity was comparable to the spleen, where we detected 22 unique clusters (Online-Fig.IX,X). In aortas, 21 clusters (~97% of all leukocytes) could be assigned to principal hematopoietic lineages (Fig.4e): We detected 10x myeloid cell clusters, thereof 3x F4/80-expressing macrophage-clusters, 3x F4/80^{neg}CD11c^{high} dendritic cell-clusters, 2x monocyte-clusters (F4/80^{neg}CD11b^{med}Ly6C$^{high/low}$), and 2x granulocyte-clusters (Ly-6G^{high} or Siglec-F^{high}). In addition, 7x T-cell clusters could be identified by the expression of the lineage markers TCR-β, TCR-γ/δ, CD4, and CD8. We identified one cluster of γ/δ-T-cells, 2x CD8^{+} T-cell clusters, one mixed CD4^{+}/CD8^{+} T-cell cluster, and one unusual TCR-β^{low} cluster (20). Within the CD4^{+} T-helper cell clusters, CD5 and Ly-6C were the main differentiating markers that allowed us to sub-separate CD4^{+} T-cells into CD5^{med}Ly6-C^{high} and CD5^{high}Ly-6C^{neg} cells. Also, we found 4x B-cell clusters, of which 3 were exclusively present in WD-fed mice, and 1x Nk-cell cluster. The relative frequency of clusters differed extensively between aorta and splenic tissue, suggesting a tissue-specific response. We next examined diet-induced changes of cluster frequencies in CD vs. WD-induced disease. While the frequency of the most parental leukocyte lineages (T-, B-, myeloid cells) did not change, we found 2 clusters only present in CD-fed mice (1,20), and 4 clusters only in WD-fed mice (4,9,19,22) (Fig.4f). 3 clusters were detectable in CD-fed mice but increased in WD-induced disease (3,6,11), whereas the frequency of one cluster (26) decreased (Online-TableVII). These data demonstrate a distinct regulation of leukocyte frequencies within, but not of, leukocyte lineages.

We next interrogated how these protein-defined clusters corresponded to transcriptionally defined clusters. Therefore, we built a Pearson correlation between normalized mRNA-expression and mean-signal intensity in CyTOF for the same cellular markers. We used three panels of targets: classical lineage markers defining B-cells (Fig.5a), T-cells (Fig.5b), and myeloid cells (Fig.5c). The resulting correlation matrices revealed a high phenotypical overlap between scRNAseq and CyTOF clusters, for instance cluster 7 in scRNAseq (macrophages) was highly correlated with CyTOF macrophage cluster 3 (F4/80^{med}CD64^{high}MHC-II^{med}, R=0.91) and cluster 9 (F4/80^{high}CD64^{med}MHC-II^{med}, R=0.91), but not with cluster 22 (dendritic cells, F4/80^{neg}CD64^{low}MHC-II^{high}CD11b^{med}, R=-0.11), suggesting the macrophage clusters in CyTOF, 3 and 9, may be included in one

scRNAseq macrophage cluster. *Vice versa*, CyTOF cluster 22 showed a correlation of R=0.72 and 0.77 with the scRNAseq clusters containing monocytes and Ly-6C^{high} monocytes, identifying these cells as myeloid-derived DCs. These data demonstrate the feasibility and superiority of higher multiplexed immuno-phenotyping in estimating the diversity and diet-induced changes of aortic leukocytes. Together with mRNA-based definition of clusters, our data help to build a cellular immune cell atlas in atherosclerosis.

Transcriptional, phenotypic, and functional profiles identify three principal aortic B-cell sub-populations

Leukocyte heterogeneity has consequences for atherosclerosis. For instance, B-cells can be pro-atherogenic (B2-like, B220^{+}CD23^{+}CD11b^{-})[15, 16] or atheroprotective (B1-like, B220^{low}CD11b^{+}CD23^{-}CD5^{+})[17]. To test whether highly multiplexed approaches can detect such intra-B-cell heterogeneity in an unsupervised manner, we filtered cellular *Cd19*-mRNA^{+} events from aortas with WD-induced atherosclerosis (Fig.6a). The filtered cells specifically expressed transcripts of B-cell markers (Fig.6b). The top 250 variable genes were used as an input for dimensionality reduction, which retrieved three B-cell populations (Fig.6c). Pathway analysis of cluster DE-genes (Fig.6d) retrieved an increase of genes involved in antigen-presentation, co-stimulation, antibody generation (‘immunity’), and cellular- adhesion and cross-talk (‘cell adhesion’) in B-cell cluster 1. The smallest cluster 2 expressed cell-division genes, while cluster 3 up-regulated apoptosis-related and pro-inflammatory TNF-signaling genes. These scRNAseq-defined B-cell clusters were distinguishable by the markers CD43 and B220 (CD43^{high}B220^{neg}, CD43^{neg}B220^{high}, CD43^{low}B220^{high}). Notably, these markers also separated B-cells in FACS (Online-TableVIII) and CyTOF (Fig.6e). Based on their transcriptome the three B-cell clusters showed differential expression of CCL5 and GM-CSF, two important mediators of atherosclerosis. We therefore quantified *in vitro* cytokine production (Fig.6f-h): The B-cell cluster CD43^{high}B220^{neg} showed higher expression of the pro-atherogenic chemokine CCL5 (RANTES), while CD43^{neg}B220^{high} expressed more of the pro-inflammatory cytokine IFN-γ. Both B220^{neg} clusters showed higher expression of GM-CSF compared to B220^{high} B-cells. Taken together, these data suggest a distinct functional role of cell clusters identified by scRNAseq/CyTOF.

The frequency of aortic leukocyte populations predicts clinical events in patients with atherosclerosis

We next aimed to clarify the composition of human atherosclerotic plaques with an anti-human antibody panel for CyTOF (TableS9) tested on leukocytes isolated from a human carotid endarterectomy specimen (Fig.7a). In contrast to histology, which has established a predominance of macrophages in human plaques, we found only a small percentage of cells assigned to the myeloid cell lineages (CD11b^{+}). Contrastingly, the heterogeneity of leukocyte populations was comparable to CyTOF of mouse aortic leukocytes with 19 clusters in total (Fig.7b). To exclude false-negative results caused by a lack of specific macrophages markers in humans or a selective death of macrophages during tissue digestion, we applied the mRNA deconvolution strategy to gene-expression arrays of 126 carotid plaques from the Biobank of Karolinska Endarterectomies (BiKE)[18] to enumerate the relative abundance of leukocyte populations (Fig.7c, Online-Fig.XI). This approach revealed

that 51.1±0.9% of all leukocytes were macrophages, 19.3±0.6% T-cells, and 13.9±0.4% monocytes. The fraction of most leukocyte populations (except for the $CD4^+/CD8^+$ T-cell- and the Nk-cell containing clusters) was relatively enriched in plaques when compared to their relative frequencies in PBMCs from the same patients, suggesting a non-random enrichment (Fig.7d). Finally, we correlated cluster frequencies in human plaques and the rate of ischemic events (IE) post endarterectomy in the same patient cohort. We found that of all tested cluster, the memory T-cell containing cluster negatively predicted cardiovascular events (Fig.7e), while the frequency of macrophages only showed a weak (positive) tendency (not shown). These results help to clarify leukocyte diversity in human plaques and suggest leukocyte composition as potential driver of adverse clinical events.

Discussion

Here, we applied novel high-dimensional methods, utilizing 35 parameters (CyTOF) and ~1100 parameters (scRNAseq) and an unsupervised subset detection strategy to define the diversity, phenotypes, and transcriptomes of leukocytes in atherosclerotic aortas. Our study demonstrates several fundamental discoveries: We resolved the relative leukocyte composition in murine atherosclerosis in a more accurate way than previously reported. Reports on conventional flow cytometry of aortic leukocytes were limited by pre-defined leukocyte panels, which only examined parental hematopoietic lineages or were focused on the heterogeneity within distinct lineages[4, 8, 19]. The limited number of markers in flow cytometry is not sufficient to deeply characterize more than one lineage at a time[7]. Using CyTOF, we assigned almost all aortic leukocytes to hematopoietic cell identities, while 17% of leukocytes remained unidentifiable by flow cytometry. We confirmed that B-cells, myeloid cells, T-cells, and others – including rare (TCR-γ/δ^+) and atypical T-cell clusters – each account for ~¼ of all leukocytes. These results are comparable to previously published frequencies of myeloid cells (~25-42%), T-cells (~21-35%), and B-cells (~13-19%) in *Apoe*$^{-/-}$ mice[4, 8]. These numbers appear to be robust despite substantial differences in feeding, tissue digestion protocols, and leukocyte panels used in earlier studies[4, 19]. CyTOF was superior in detecting smaller populations, such as TCRγ/δ T-cells that accounted for only ~1% of leukocytes. Sub-lineage heterogeneity, i.e. the sub-separation of lineages in distinct phenotypes, was surprisingly high in aortic leukocytes (23 CyTOF-defined clusters) and equivalent to the spleen (22 clusters). While B-cells were the dominant leukocyte subset in the spleen (8 cluster accounting for ~42% of leukocytes), T-cell and myeloid cell clusters dominated aortic leukocytes in mouse and human atherosclerotic lesions based on genetic deconvolution. The higher number of clusters retrieved by CyTOF was likely caused by the pre-defined panel of surface markers with a known high variability within lineages, whereas scRNAseq algorithms aim to detect differences in the whole transcriptome and thereby may neglect cellular entities with a few distinct protein markers only. Based on our approach to integrate CyTOF and scRNAseq, we were able to define some hallmarks of leukocyte diversity and dynamics in atherosclerosis (Online-Fig.XII):

T-cells

T-cells represented the second most frequent population in healthy arterial tissue. Of the three pure $CD4^+$ T-cell clusters in scRNAseq, one cluster was transcriptionally similar to

memory T-cells and showed a WD-induced enrichment of cell cycle genes, suggestive of a tissue-specific proliferative response. Lately, tissue-resident memory T cells within non-lymphoid organs have been identified. These persist in tissue after viral or bacterial infection and show a strong tissue-restricted response after re-activation with their cognate antigen[20]. Notably, we observed that the absence of this T-cell subset significantly correlated with increased risk to develop an ischemic event in patients, suggesting an overall protective function. The frequency of this memory-like T-cell population was outnumbered by the T_H17-cell cluster. T_H17 cells have mostly been attributed to a pro-atherogenic phenotype[21-23] and seem to represent the predominant T_H-lineage induced by atherosclerosis-related antigens besides T_H1[2]. Some reports also suggested a regulatory, atheroprotective role[24]. Whether T_H2-polarized T-cells, which we detected in the third $CD4^+$ T-cell cluster, are important in atherosclerosis is controversial[2]. CyTOF of aortic leukocytes detected two $CD4^+$ T-cell clusters: $CD5^{med}Ly6\text{-}C^{high}$ (15) and $CD5^{high}Ly\text{-}6C^{neg}$ (17). Interestingly, we observed the same pattern of low *Cd5* and high *Ly6c1* gene expression in the memory-like RNAseq cluster, while the T_H17 cluster had an inverted pattern. Notably, Ly6-C can be a marker of memory T-cells. During viral infection, memory T-cells stem from a $Ly6\text{-}C^+$ T-helper cell subset[25]. Contrastingly, Ly-6C was also described as marker of a smaller subset of T_{regs} with a weakened immunosuppressive capacity[26]. In both subsets, in scRNAseq and CyTOF, CD5 expression was inversely correlated to Ly6-C. The expression level of CD5 is known to correlate with T-cell receptor (TCR) signaling events and antigen-induced proliferation[27]. CD5 is also highly expressed on induced T_{regs} that less suppressive and prone to turn into a T-effector cell[28]. In addition, CD5 is known as survival factor for T cells. For instance, tumor infiltrating $CD5^+$ T-cells downregulate the apoptosis inducing factor FasL[29, 30] and induce CK2-dependent survival pathways[31]. Both T-helper cell subsets also expressed folate receptor 4 (FR4), a marker of protective T-regulatory cells (T_{regs})[32]. The absence of the T_{reg}-defining marker CD25 (IL-2 receptor)[33] suggest that both clusters, however, may be central memory or effector-memory T-cells[34]. This is also supported by the observation that antigen-stimulated $CD4^+$ T-cells up-regulate FR4 and down-regulate CD25[32]. Collectively, these findings render the main T-cell subsets in the atherosclerotic aorta as effector or central-memory and likely not regulatory T-cells, which is consistent with a loss of T_{regs} in the plaque[35] likely caused by a phenotypic conversion into effector T-cells[36]. Whether the memory-like T-cell cluster found in healthy aortas represents a type of tissue-resident T-cells cannot be answered by our dataset. As well, the functional contribution of $CD4^+$ T-cell expressed CD5, FR4, or Ly6-C to atherosclerosis is unknown and will require studies with T-helper cell specific knock-outs.

B cells

$CD19^+$ B-cells were already detectable in healthy arteries, likely in the adventitia, where we detected a robust B-cell specific gene signal with our genetic deconvolution approach, while in late atherosclerosis, B-cells predominantly populated ATLOs as suggested before[37]. Contrastingly, in atherosclerotic lesions, both in mice and humans, we found B-cells only in minor frequencies, thus, indicating that conventional flow cytometry from whole atherosclerotic aortas overestimates the actual B-cell-content. CyTOF of atherosclerotic aortas identified a B2-like cell cluster that expanded in WD-fed mice and may therefore reflect a pro-atherosclerotic subset, while the B1-like cell clusters 1 and 13 were found in

lower quantities in atherosclerotic lesions, consistent with the proposed atheroprotective function of B1-cells[17]. However, the marker-based categorization in known subsets with established functions may not be entirely appropriate: In a sub-clustering approach of *Cd19*-mRNA^{+} cells in scRNAseq we found three distinct clusters. One cluster that matched the core marker profile of B1-cells (CD43^{high}B220^{neg}CD11b^{high}), but showed an enrichment for TNF-signaling and cell adhesion pathways, validated by a strong secretion of the chemokine CCL5. Notably, B-cell-specific deletion of TNF-α reduced atherosclerosis and plaque vulnerability, rendering these cells as likely pro-atherogenic[38]. The other two B-cell clusters with a surface marker profile of pro-atherogenic B2-cells[39] secreted the known pro-atherogenic mediators IFN-γ and GM-CSF.

Myeloid cells

In scRNAseq, healthy arterial tissue was pre-dominantly populated by macrophages that co-expressed markers of the previously reported arterial, tissue-resident *Cx3cr1*$^{+}$ macrophage subset. Interestingly, the expression of *Cx3cr1* and *Lyve1* on aortic macrophages was maintained throughout atherosclerosis, raising the general question to which extend the macrophage pool is replenished from monocytes or depending on *in situ* proliferation as previously suggested[40]. Interestingly, the fraction of monocytes in the aorta was relatively higher in healthy tissue, comprised mainly of Ly6C^{+} inflammatory monocytes, and decreased in disease. Among all monocytes in the atherosclerotic aorta, Ly-6C^{low} monocytes overwhelmed their Ly6C^{high} counterparts. The latter, however, was significantly enriched in genes associated with acute myocardial infarction, which proposes a role of these cells in clinical disease.

Limitations

One limitation of the current study and of previous reports is that we assessed the leukocyte distribution in whole aortas, which represents a mixture of phenotypically and likely biologically distinct lesions from atherosclerotic plaques, plaque-free parts of the aorta, developing atheroma, and fatty streaks, and may affect leukocyte composition, in particular in comparison to human carotid or coronary atherosclerotic lesions. Currently, the only technique to isolate plaque specific areas is laser capture microdissection[41], which yields insufficient cells for FACS, CyTOF, and scRNA-Seq. It is likely that leukocyte phenotypes may depend on their temporal and spatial distribution. For instance, it is known that leukocytes accumulate at different sites in healthy and atherosclerotic aortas. While macrophages and macrophage-derived foam cells are predominantly found in atherosclerotic plaques[2], B-cells are thought to primarily reside in the adventitia, or at later stages, in tertiary lymphoid organs[37]. However, we have circumvented this limitation by using a novel gene-expression deconvolution method with gene signatures specific for aortic leukocytes. These data establish a predominant accumulation of myeloid cells and T-cells in microdissected mouse plaques and human carotid plaques, while B cells predominate adventitial tissue and are only found in minor frequencies in plaques. In this regard, flow cytometry of whole mouse aortas is incapable of estimating the actual cellular composition of the plaque.

To define specific markers is a prerequisite of CyTOF and flow cytometry, which may limit the detection of some human lesional leukocytes. For instance, some well-established macrophage markers in the mouse are either not translatable (F4/80) or less specific for human plaque macrophages (CD69, CD68, MERTK). This is consistent with our observation that in CyTOF of leukocytes from human lesions only a minor fraction of was identified as $CD11b^{+}$ myeloid cells, which is in contrast to their reported high frequencies in histology. Also, the prolonged digestion and mechanical disruption of often calcified human plaques may contribute to a selective loss of some more fragile leukocyte subsets.

scRNAseq can bypass some of these limitations for CyTOF but has an inferior sensitivity to detect cellular clusters: Cells with a similar transcriptional program as consequence of a tissue wide biological response may be grouped in dimensionality reduction plots and thereby falsely regarded as the same population. Complementary strategies by integrating marker expression (protein), marker gene transcripts (mRNA), and pathways (gene set enrichment of differentially expressed genes) as reported here, however, may limit such effects.

Translational aspects

The identification of aortic/lesional and specialized leukocyte subpopulations has greatly advanced atherosclerosis research in the last decades, but the relevance of these findings for human disease remains puzzling[2]. Conventional flow cytometry of whole atherosclerotic mouse aortas has yielded inconsistent results compared to the leukocyte composition of human plaques. While the partial lack of translatable cellular markers and the use of the likely biased $Apoe^{-/-}$ and $Ldlr^{-/-}$ mouse models may explain some of this inconsistency, site-specific accumulation of leukocytes and the inability to isolate sufficient numbers of leukocytes from mouse plaques for immune-phenotyping represents another important limitation. By employing a novel deconvolution strategy based on single cell transcriptomes, we show that the cellular composition of mouse and human plaques is almost identical and relatively dominated by macrophages and myeloid cells (~60-75%) and T-cells (~25%). In addition, our study proposes that frequencies and the gene expression of lesional leukocyte may have the potential to serve as supplementary risk stratification tool. Gene expression deconvolution methods have opened the avenue to virtually construct the leukocyte repertoire in gene expression data from biopsies in cancer[10] and specific changes in gene expression sets from carotid plaque specimen associate with clinical outcomes[18]. Although coronary plaque samples are not available on a routine basis, such cellular biomarkers could improve risk prediction tools, which will be of great value for emerging personalized therapies in future cardiovascular medicine.

Our findings show that the immune cell landscape in atherosclerosis is unexpectedly diverse, relatively dominated by T-cell and myeloid cells, and highly selectively regulated. Besides the methodological novelty of our work, our data directly propose the existence of several novel leukocyte subsets that were not detected by traditional technology. Additionally, our data represent a useful resource for future functional work in which subsets described herein are manipulated by Cre-lox, adoptive transfers, or depletion approaches. The design of specific surface marker panels to define aortic leukocyte subsets may yield useful

biomarkers to assess progression and regression of atherosclerosis, and to predict plaque vulnerability, which correlates with clinical events.

Supplementary Material

Refer to Web version on PubMed Central for supplementary material.

Acknowledgments

We thank Cheryl Kim, Lara Boggeman, Denise Hinz, and Robin Simmons for help with flow sorting and Kristen Jepsen for the help with single cell RNA-sequencing. We thank Angela Denn for histology and microscopy. This work was supported by grants to D. Wolf from the Deutsche Forschungsgemeinschaft (DFG WO1994/1). K. Ley was supported by grants HL115232, HL88093, and HL121697 from the National Heart, Lung, and Blood Institute. The CyTOF Helios Mass Cytometer and the FACS-Aria-3 cell sorter were supported by the Shared Instrumentation Grant (SIG) Program S10 OD018499-01 and RR027366-01A1, respectively.

Non-Standard Abbreviations and Acronyms

scRNAseq	Single-cell RNA sequencing
CyTOF	Cytometry by Time of Flight (mass cytometry)
WD	Western diet
CD	Chow diet
T_H1	Type 1 T-helper cell
T_{reg}	T-regulatory cell
ATLO	Artery tertiary lymphoid organ
FACS	Fluorescence-activated cell sorting
GD	Genetic deconvolution
tSNE	t-distributed stochastic neighbor embedding

References

1. Libby P. Inflammation in atherosclerosis. Nature. 2002; 420:868–874. [PubMed: 12490960]
2. Wolf D, Zirlik A, Ley K. Beyond vascular inflammation–recent advances in understanding atherosclerosis. Cell Mol Life Sci. 2015; 72:3853–3869. [PubMed: 26100516]
3. Weber C, Zernecke A, Libby P. The multifaceted contributions of leukocyte subsets to atherosclerosis: Lessons from mouse models. Nat Rev Immunol. 2008; 8:802–815. [PubMed: 18825131]
4. Galkina E, Kadl A, Sanders J, Varughese D, Sarembock IJ, Ley K. Lymphocyte recruitment into the aortic wall before and during development of atherosclerosis is partially l-selectin dependent. J Exp Med. 2006; 203:1273–1282. [PubMed: 16682495]
5. Spitzer MH, Carmi Y, Reticker-Flynn NE, Kwek SS, Madhireddy D, Martins MM, Gherardini PF, Prestwood TR, Chabon J, Bendall SC, Fong L, Nolan GP, Engleman EG. Systemic immunity is required for effective cancer immunotherapy. Cell. 2017; 168:487–502 e415. [PubMed: 28111070]
6. Villani AC, Satija R, Reynolds G, Sarkizova S, Shekhar K, Fletcher J, Griesbeck M, Butler A, Zheng S, Lazo S, Jardine L, Dixon D, Stephenson E, Nilsson E, Grundberg I, McDonald D, Filby A, Li W, De Jager PL, Rozenblatt-Rosen O, Lane AA, Haniffa M, Regev A, Hacohen N. Single-cell

rna-seq reveals new types of human blood dendritic cells, monocytes, and progenitors. Science. 2017; 356

7. Bjornson ZB, Nolan GP, Fantl WJ. Single-cell mass cytometry for analysis of immune system functional states. Curr Opin Immunol. 2013; 25:484–494. [PubMed: 23999316]
8. Butcher MJ, Herre M, Ley K, Galkina E. Flow cytometry analysis of immune cells within murine aortas. J Vis Exp. 2011
9. Chen Z, Huang A, Sun J, Jiang T, Qin FX, Wu A. Inference of immune cell composition on the expression profiles of mouse tissue. Sci Rep. 2017; 7:40508. [PubMed: 28084418]
10. Newman AM, Liu CL, Green MR, Gentles AJ, Feng W, Xu Y, Hoang CD, Diehn M, Alizadeh AA. Robust enumeration of cell subsets from tissue expression profiles. Nat Methods. 2015; 12:453–457. [PubMed: 25822800]
11. Grabner R, Lotzer K, Dopping S, Hildner M, Radke D, Beer M, Spanbroek R, Lippert B, Reardon CA, Getz GS, Fu YX, Hehlgans T, Mebius RE, van der Wall M, Kruspe D, Englert C, Lovas A, Hu D, Randolph GJ, Weih F, Habenicht AJ. Lymphotoxin beta receptor signaling promotes tertiary lymphoid organogenesis in the aorta adventitia of aged apoe−/− mice. J Exp Med. 2009; 206:233–248. [PubMed: 19139167]
12. Mills CD, Ley K. M1 and m2 macrophages: The chicken and the egg of immunity. J Innate Immun. 2014; 6:716–726. [PubMed: 25138714]
13. Szelag M, Piaszyk-Borychowska A, Plens-Galaska M, Wesoly J, Bluyssen HA. Targeted inhibition of stats and irfs as a potential treatment strategy in cardiovascular disease. Oncotarget. 2016; 7:48788–48812. [PubMed: 27166190]
14. Mallat Z, Gojova A, Marchiol-Fournigault C, Esposito B, Kamate C, Merval R, Fradelizi D, Tedgui A. Inhibition of transforming growth factor-beta signaling accelerates atherosclerosis and induces an unstable plaque phenotype in mice. Circ Res. 2001; 89:930–934. [PubMed: 11701621]
15. Kyaw T, Tay C, Khan A, Dumouchel V, Cao A, To K, Kehry M, Dunn R, Agrotis A, Tipping P, Bobik A, Toh BH. Conventional b2 b cell depletion ameliorates whereas its adoptive transfer aggravates atherosclerosis. J Immunol. 2010; 185:4410–4419. [PubMed: 20817865]
16. Ait-Oufella H, Herbin O, Bouaziz JD, Binder CJ, Uyttenhove C, Laurans L, Taleb S, Van Vre E, Esposito B, Vilar J, Sirvent J, Van Snick J, Tedgui A, Tedder TF, Mallat Z. B cell depletion reduces the development of atherosclerosis in mice. J Exp Med. 2010; 207:1579–1587. [PubMed: 20603314]
17. Kyaw T, Tay C, Krishnamurthi S, Kanellakis P, Agrotis A, Tipping P, Bobik A, Toh BH. B1a b lymphocytes are atheroprotective by secreting natural igm that increases igm deposits and reduces necrotic cores in atherosclerotic lesions. Circ Res. 2011; 109:830–840. [PubMed: 21868694]
18. Folkersen L, Persson J, Ekstrand J, Agardh HE, Hansson GK, Gabrielsen A, Hedin U, Paulsson-Berne G. Prediction of ischemic events on the basis of transcriptomic and genomic profiling in patients undergoing carotid endarterectomy. Mol Med. 2012; 18:669–675. [PubMed: 22371308]
19. Gjurich BN, Taghavie-Moghadam PL, Galkina EV. Flow cytometric analysis of immune cells within murine aorta. Methods Mol Biol. 2015; 1339:161–175. [PubMed: 26445788]
20. Mueller SN, Mackay LK. Tissue-resident memory t cells: Local specialists in immune defence. Nat Rev Immunol. 2016; 16:79–89. [PubMed: 26688350]
21. Smith E, Prasad KM, Butcher M, Dobrian A, Kolls JK, Ley K, Galkina E. Blockade of interleukin-17a results in reduced atherosclerosis in apolipoprotein e-deficient mice. Circulation. 2010; 121:1746–1755. [PubMed: 20368519]
22. Gao Q, Jiang Y, Ma T, Zhu F, Gao F, Zhang P, Guo C, Wang Q, Wang X, Ma C, Zhang Y, Chen W, Zhang L. A critical function of th17 proinflammatory cells in the development of atherosclerotic plaque in mice. J Immunol. 2010; 185:5820–5827. [PubMed: 20952673]
23. Taleb S, Tedgui A, Mallat Z. Il-17 and th17 cells in atherosclerosis: Subtle and contextual roles. Arterioscler Thromb Vasc Biol. 2015; 35:258–264. [PubMed: 25234818]
24. Taleb S, Romain M, Ramkhelawon B, Uyttenhove C, Pasterkamp G, Herbin O, Esposito B, Perez N, Yasukawa H, Van Snick J, Yoshimura A, Tedgui A, Mallat Z. Loss of socs3 expression in t cells reveals a regulatory role for interleukin-17 in atherosclerosis. J Exp Med. 2009; 206:2067–2077. [PubMed: 19737863]

25. Marshall HD, Chandele A, Jung YW, Meng H, Poholek AC, Parish IA, Rutishauser R, Cui W, Kleinstein SH, Craft J, Kaech SM. Differential expression of ly6c and t-bet distinguish effector and memory th1 cd4(+) cell properties during viral infection. Immunity. 2011; 35:633–646. [PubMed: 22018471]
26. Delpoux A, Yakonowsky P, Durand A, Charvet C, Valente M, Pommier A, Bonilla N, Martin B, Auffray C, Lucas B. Tcr signaling events are required for maintaining cd4 regulatory t cell numbers and suppressive capacities in the periphery. J Immunol. 2014; 193:5914–5923. [PubMed: 25381435]
27. Mandl JN, Monteiro JP, Vrisekoop N, Germain RN. T cell-positive selection uses self-ligand binding strength to optimize repertoire recognition of foreign antigens. Immunity. 2013; 38:263–274. [PubMed: 23290521]
28. Henderson JG, Opejin A, Jones A, Gross C, Hawiger D. Cd5 instructs extrathymic regulatory t cell development in response to self and tolerizing antigens. Immunity. 2015; 42:471–483. [PubMed: 25786177]
29. Ryan KR, McCue D, Anderton SM. Fas-mediated death and sensory adaptation limit the pathogenic potential of autoreactive t cells after strong antigenic stimulation. J Leukoc Biol. 2005; 78:43–50. [PubMed: 15817704]
30. Friedlein G, El Hage F, Vergnon I, Richon C, Saulnier P, Lecluse Y, Caignard A, Boumsell L, Bismuth G, Chouaib S, Mami-Chouaib F. Human cd5 protects circulating tumor antigen-specific ctl from tumor-mediated activation-induced cell death. J Immunol. 2007; 178:6821–6827. [PubMed: 17513730]
31. Axtell RC, Xu L, Barnum SR, Raman C. Cd5-ck2 binding/activation-deficient mice are resistant to experimental autoimmune encephalomyelitis: Protection is associated with diminished populations of il-17-expressing t cells in the central nervous system. J Immunol. 2006; 177:8542–8549. [PubMed: 17142752]
32. Yamaguchi T, Hirota K, Nagahama K, Ohkawa K, Takahashi T, Nomura T, Sakaguchi S. Control of immune responses by antigen-specific regulatory t cells expressing the folate receptor. Immunity. 2007; 27:145–159. [PubMed: 17613255]
33. Wu Y, Borde M, Heissmeyer V, Feuerer M, Lapan AD, Stroud JC, Bates DL, Guo L, Han A, Ziegler SF, Mathis D, Benoist C, Chen L, Rao A. Foxp3 controls regulatory t cell function through cooperation with nfat. Cell. 2006; 126:375–387. [PubMed: 16873067]
34. Walker LS. Regulatory t cells: Folate receptor 4: A new handle on regulation and memory? Immunol Cell Biol. 2007; 85:506–507. [PubMed: 17710105]
35. Maganto-Garcia E, Tarrio ML, Grabie N, Bu DX, Lichtman AH. Dynamic changes in regulatory t cells are linked to levels of diet-induced hypercholesterolemia. Circulation. 2011; 124:185–195. [PubMed: 21690490]
36. Li J, McArdle S, Gholami A, Kimura T, Wolf D, Gerhardt T, Miller J, Weber C, Ley K. Ccr5+t-bet +foxp3+ effector cd4 t cells drive atherosclerosis. Circ Res. 2016; 118:1540–1552. [PubMed: 27021296]
37. Srikakulapu P, Hu D, Yin C, Mohanta SK, Bontha SV, Peng L, Beer M, Weber C, McNamara CA, Grassia G, Maffia P, Manz RA, Habenicht AJ. Artery tertiary lymphoid organs control multilayered territorialized atherosclerosis b-cell responses in aged apoe−/− mice. Arterioscler Thromb Vasc Biol. 2016; 36:1174–1185. [PubMed: 27102965]
38. Tay C, Liu YH, Hosseini H, Kanellakis P, Cao A, Peter K, Tipping P, Bobik A, Toh BH, Kyaw T. B-cell-specific depletion of tumour necrosis factor alpha inhibits atherosclerosis development and plaque vulnerability to rupture by reducing cell death and inflammation. Cardiovasc Res. 2016; 111:385–397. [PubMed: 27492217]
39. Kyaw T, Tipping P, Toh BH, Bobik A. Current understanding of the role of b cell subsets and intimal and adventitial b cells in atherosclerosis. Curr Opin Lipidol. 2011; 22:373–379. [PubMed: 21881498]
40. Hilgendorf I, Swirski FK, Robbins CS. Monocyte fate in atherosclerosis. Arterioscler Thromb Vasc Biol. 2015; 35:272–279. [PubMed: 25538208]
41. Feig JE, Fisher EA. Laser capture microdissection for analysis of macrophage gene expression from atherosclerotic lesions. Methods Mol Biol. 2013; 1027:123–135. [PubMed: 23912984]

Novelty and Significance

What Is Known?

- The growth of atherosclerosis lesions is regulated by the interplay and accumulation of pro- and anti-inflammatory leukocytes in the arterial wall.
- Traditional methods, such as flow cytometry and histology, are not sufficient to depicting the actual, large diversity of the immune cell landscape in inflammation.

What New Information Does This Article Contribute?

- State-of-the-art highly multiplexed immune-phenotyping by mass cytometry and single-cell RNA-sequencing identifies an unexpected high heterogeneity of arterial leukocytes in atherosclerosis.
- Clusters of arterial leukocytes differ in surface-markers, genetic programs, and cytokine secretion, are differentially regulated in healthy and atherosclerotic arteries, and accumulate at distinct locations within the arterial wall.
- The computation of genetic signatures obtained by single-cell RNA-sequencing reveals macrophages, T-cells, and monocytes as the main cellular components in mouse and human atherosclerotic plaques.

Atherosclerosis is a lipid-driven chronic inflammatory disease that depends on the interplay of different hematopoietic lineages in the atherosclerotic aorta and the plaque. Although leukocytes in the plaques impact on disease progression, the phenotypic and transcriptional diversity of aortic leukocytes is not well defined by conventional methods. By applying the high-perplexity methods mass cytometry and single-cell RNA-sequencing we find that the immune cell landscape in atherosclerosis is unexpectedly diverse and highly regulated. An integrated approach combining surface markers, signature genes, genetic pathways, and cytokine secretion by clusters of leukocytes with similar phenotypes defines an atlas of the immune cell repertoire in atherosclerosis. This approach descrambles the regulation and location of cells in mouse and human atherosclerosis and demonstrates that cellular subsets in the atherosclerotic plaque may predict adverse cardiovascular events in patients at risk. Our data represent a valuable resource for vascular research and will ultimately help opening up a new avenue of immunological research in atherosclerosis.

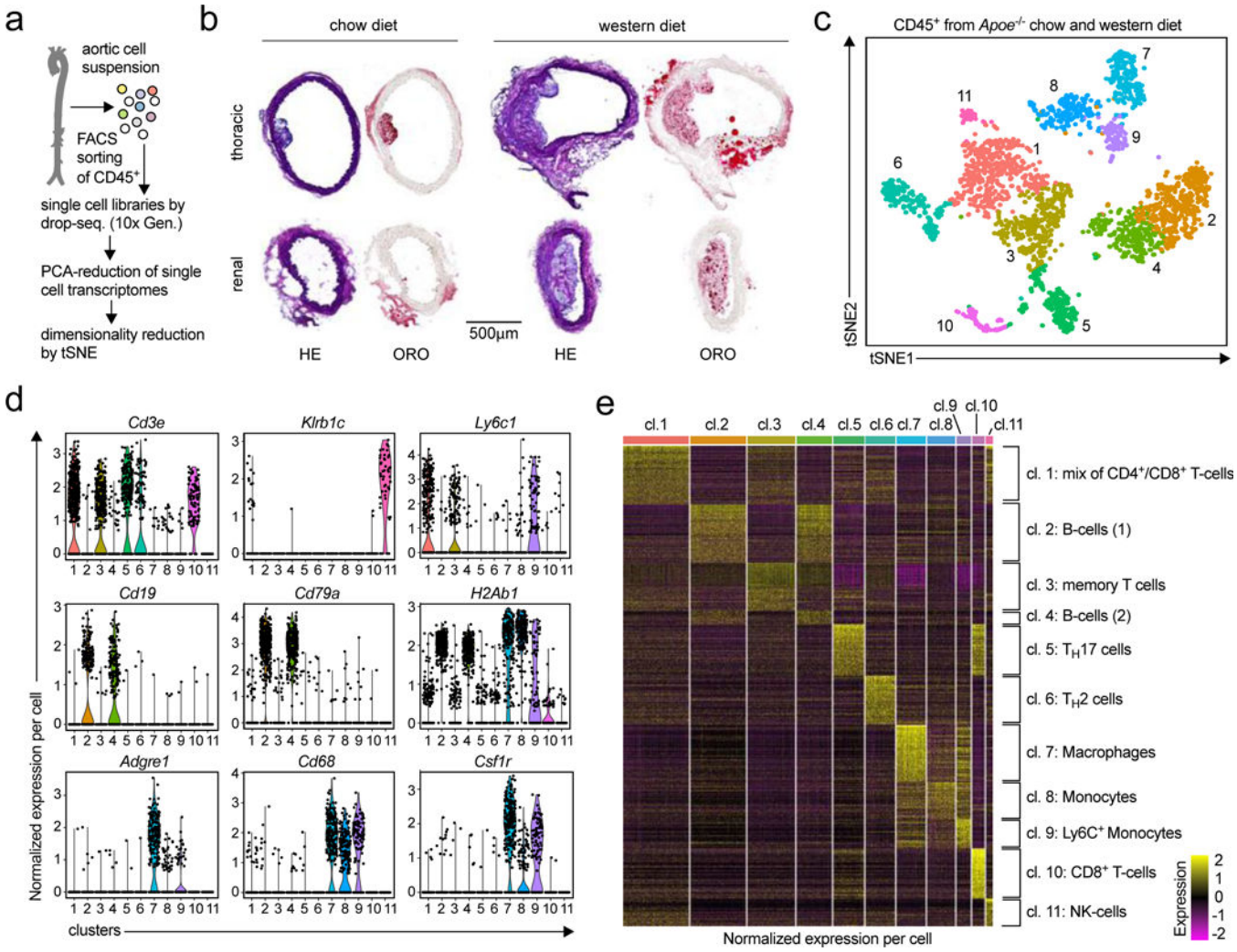

Figure 1. The single cell transcriptome identifies 11 distinct leukocyte populations in the atherosclerotic aorta

(**a**) The workflow for single cell RNA-sequencing (scRNAseq) included cell isolation of aortic leukocytes, flow sorting, and drop-sequencing. (**b**) 8-week old, female *Apoe*$^{-/-}$ mice consumed either a chow (CD) or a western diet (WD) for 12 weeks. Cross-sections of the thoracic and renal aorta were stained with hematoxylin and eosin (H&E) to display cellularity or Oil-Red-O (ORO) to assess lipid depositions. (**c**) Single cell transcriptomes of aortic leukocytes from CD and WD-fed mice were analyzed with an unsupervised dimensionality reduction algorithm (SEURAT) to identify groups of cells with similar gene expression. (**d**) Expression of principal hematopoietic lineage markers in the eleven identified cell clusters shown as normalized gene expression per cell. (**e**) Top 500 differentially expressed genes among all detected aortic leukocyte clusters. Normalized single cell gene expression is shown. Retrieved clusters were assigned to known leukocyte lineages by an integrated analysis of lineage markers and the comparison to published mouse PBMC gene signatures (Online-Fig.IV). 10 aortas from *Apoe*$^{-/-}$ mice per group were included in the pool of leukocytes (**c-f**). Representative sections are shown in (**b**).

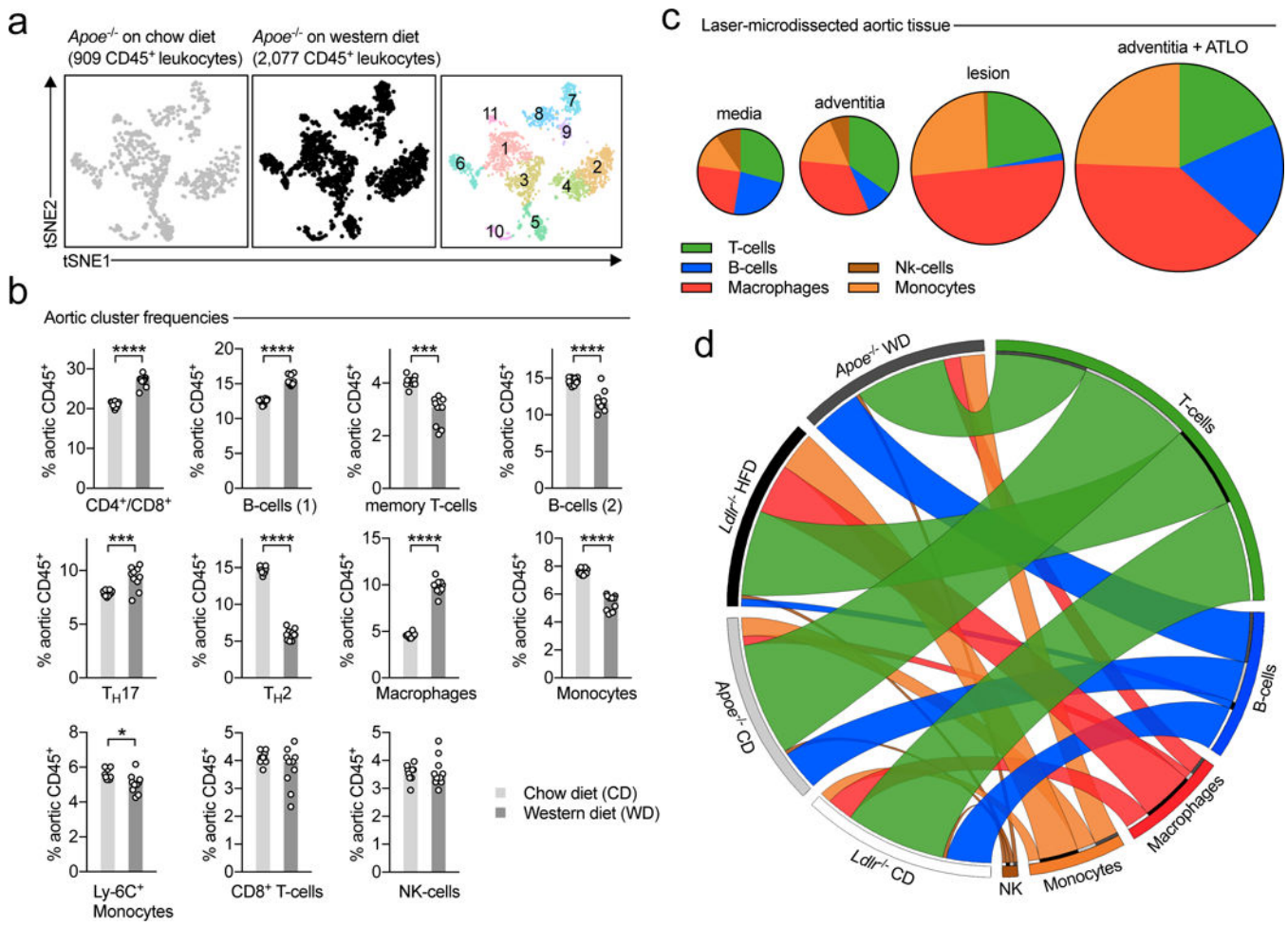

Figure 2. Spatial and numeric differences in the aortic leukocyte repertoire in atherosclerosis

8-week old, female *Apoe*-deficient (*Apoe*$^{-/-}$) mice consumed either a standard chow diet (CD) or a cholesterol-rich western diet (WD) for 12 weeks. Aortic leukocytes were isolated, subjected to scRNAseq, and distinct leukocyte clusters in CD and WD-fed mice were identified by dimensionality reduction of single cell transcriptomes. (**a**) tSNE plot for aortic leukocytes from CD (left) and WD (middle) consuming mice. Principal leukocyte clusters are displayed on the right graph. (**b**) Frequencies of the eleven clusters among all CD45^{+} leukocytes in both dietary interventions. (**c**) To characterize spatial differences of the identified leukocyte clusters, we applied a deconvolution algorithm on bulk mRNA arrays from micro-dissected tissue specimen that were obtained from female *Apoe*$^{-/-}$ mice on WD (GSE21419) and enumerated the relative frequency of the according leukocyte clusters (grouped in principal hematopoietic lineages) within the different locations. The relative proportion is shown in cake diagrams. The size of diagrams corresponds to the overall leukocyte content. (**d**) To compare the specific impact of the pro-atherogenic *Apoe*$^{-/-}$ background on leukocyte composition, we compared our results to scRNAseq on aortic leukocytes from healthy or atherosclerotic *Ldlr*$^{-/-}$ mice. Relative proportions of major hematopoietic lineages within the four combinations of dietary intervention and genotypes are displayed as Circos plot. Data are presented as mean±SEM. 10 aortas from *Apoe*$^{-/-}$ mice

per group were included in the pool of leukocytes (**b,d**). Statistical significance was assessed by a two-sided, unpaired Student's T-test on multiple iterations (**b**). *P<0.05, ***P<0.001, ****P<0.0001. DC: dendritic cells, ATLO: arterial tertiary lymphoid organs.

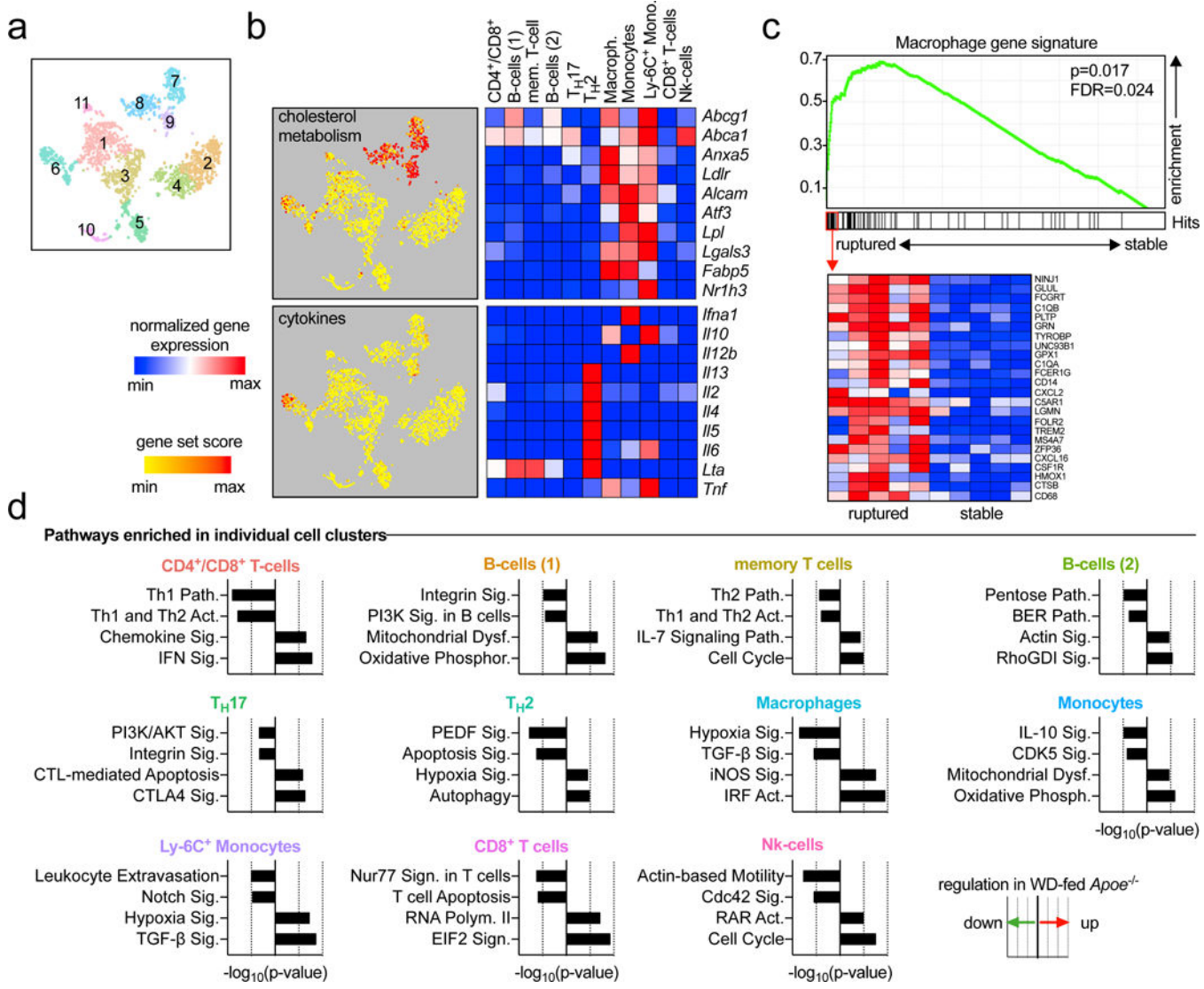

Figure 3. Enrichment of distinct genetic pathways in aortic leukocyte populations

Single cell transcriptomes of the eleven identified leukocyte clusters (**a**) were analyzed for the enrichment of specific genes and pathways. (**b**) The expression of genes contributing to cholesterol metabolism (GSEA M5892, upper graph) and cytokine secretion (GSEA M6910, lower graph) was retrieved and summarized as gene set score (specific enrichment normalized for background) per cell. Gene set scores were overlaid on single cells on a tSNE plot to identify leukocyte clusters with an enrichment of the indicated gene sets. The mean expression of some key genes in the specified gene sets is presented as heatmap with a row min.-max. score (left). (**c**) To establish a relationship between cluster gene expression and clinical disease, the enrichment of differentially expressed (DE) cluster genes compared to all other clusters was tested on bulk mRNA arrays of stable and ruptured human plaques (GSE41571) in a gene set enrichment analysis (GSEA). The specific genetic repertoire of the macrophage cluster is shown. (**d**) To identify the regulation of specific pathways between CD and WD for each individual cluster, DE genes were subjected to Ingenuity Pathway

Analysis (IPA) with a significance threshold of $P<0.05$. The top 2 down- and upregulated pathways are displayed.

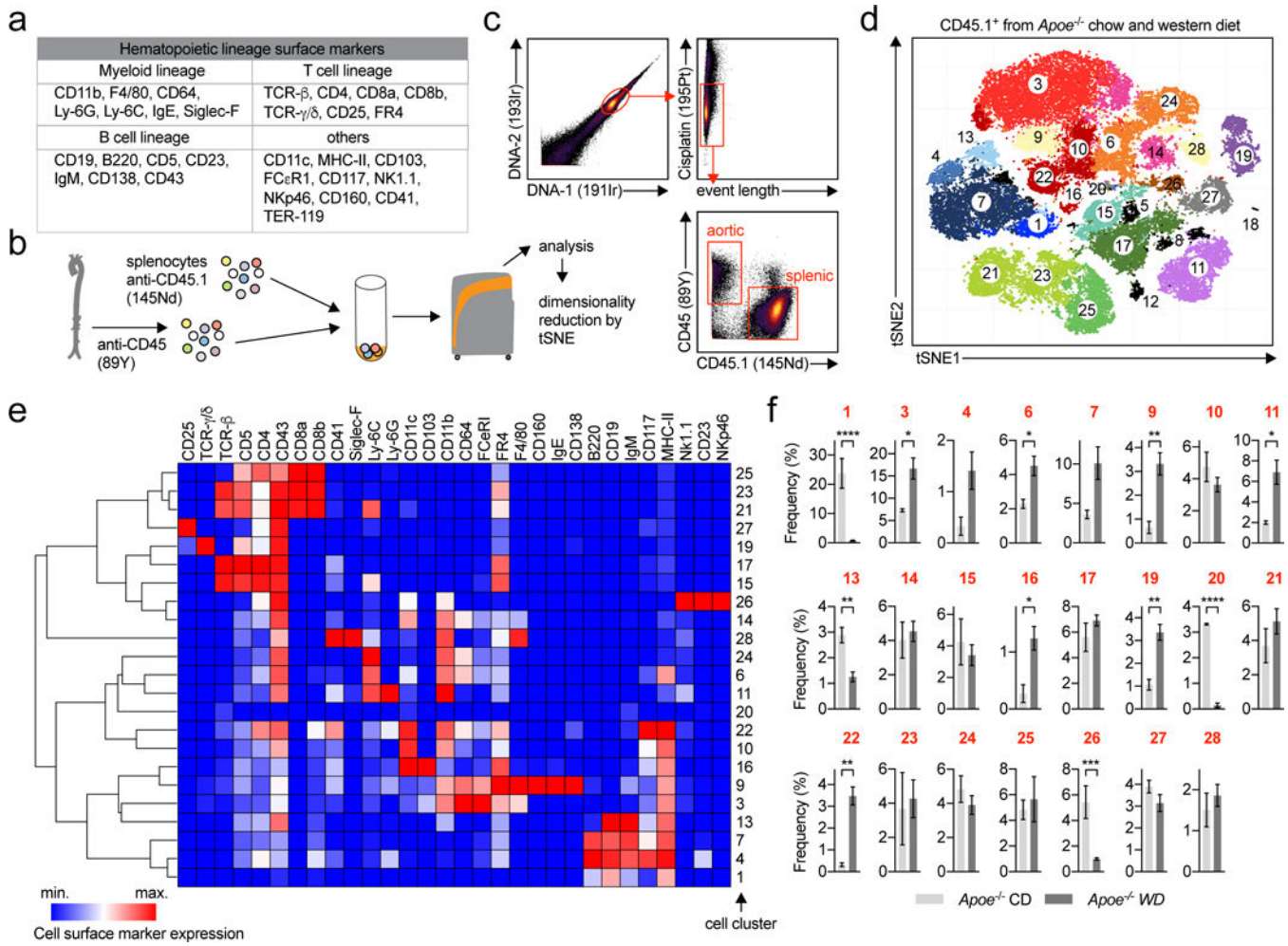

Figure 4. Mass cytometry (CyTOF) confirms the phenotypical heterogeneity of aortic leukocytes

(**a**) Markers of the 35-marker pan-leukocyte CyTOF antibody panel (full panel shown in Online-TableVI). (**b**) Aortic leukocytes were stained with an anti-CD45-89Y antibody and spiked with anti-CD45.1-145Nd stained splenocytes (1×10^6) from age-matched CD45.1 *Apoe*$^{-/-}$ mice. (**c**) Gating strategy to select viable, aortic CD45.2$^+$ leukocytes. (**d**) Unsupervised cell cluster detection by a modified tSNE and CyTOF cluster detection algorithm (PhenoGraph) on aortic leukocytes from *Apoe*$^{-/-}$ mice fed a WD or a CD. All cells in all mice are shown from a total of n=3 (CD) and n=7 (WD) mice. Macrophages are colored in red, myeloid/dendritic cells (CD11b$^{low\text{-}high}$/CD11c^{high}) in orange, T-cells (TCR-β^{high}/-γ/δ^{high} or CD4$^{low\text{-}high}$/CD8^{high}) in green/purple, B-cells (CD19^{high}) in blue, granulocytes (Ly-6G^{high}/Siglec-F^{high}) in yellow/light purple, Nk-cells (Nk1.1^{high}) in brown. (**e**) Hierarchical clustered (column and row) heatmap (column min.-max. score) of median marker expression across clusters. (**f**) Frequency of all 25 clusters in CD- and WD-fed mice above the frequency threshold of 1% (in both diets). Data are presented as mean±SEM. Significance was determined by a two-sided, unpaired Students T-test. *P<0.05, **P<0.01, ***P<0.001, ****P<0.0001. Representative CyTOF plots are shown in (**c**).

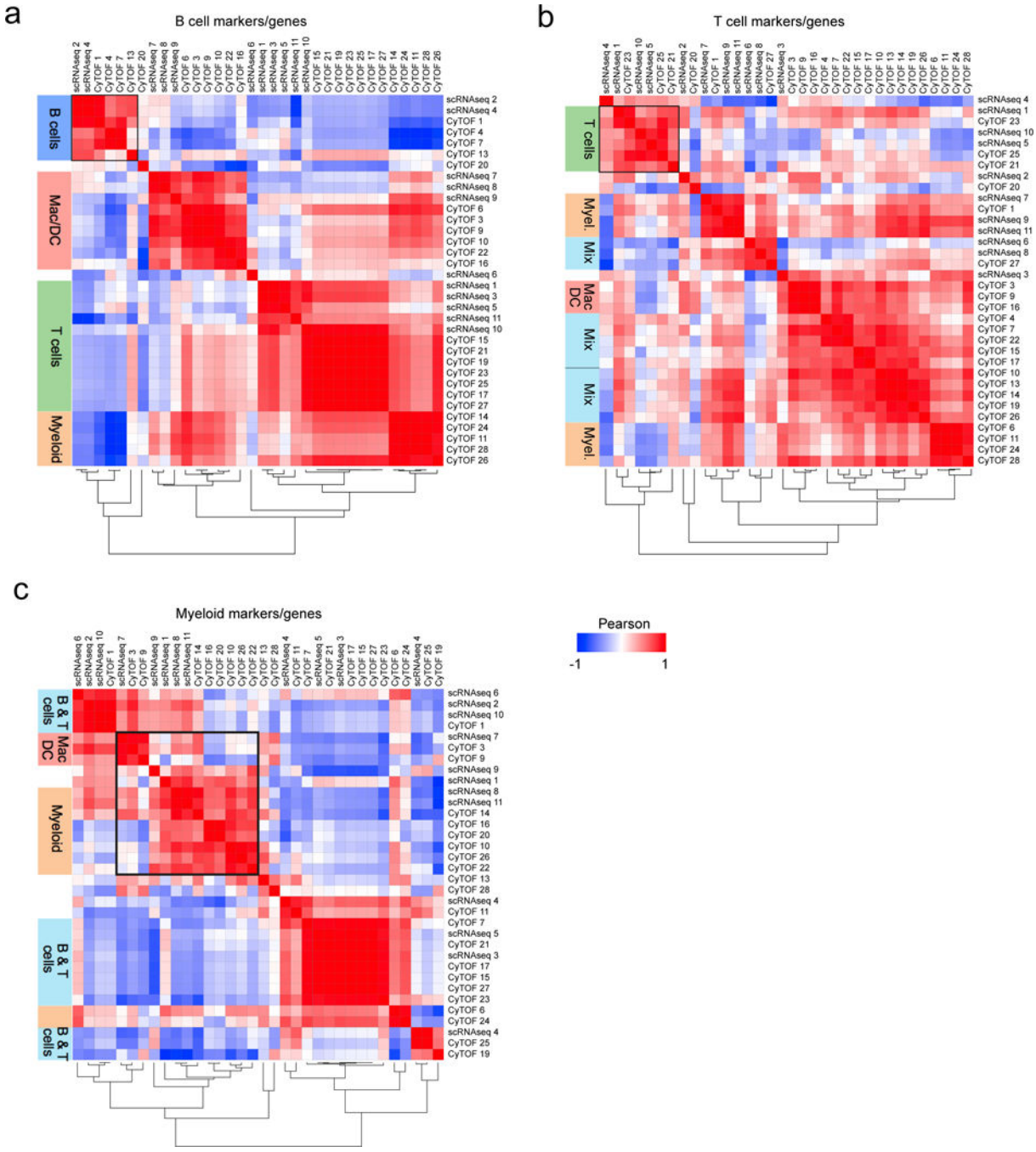

Figure 5. Leukocyte clusters identified in scRNAseq and CyTOF express highly correlated patterns of gene and protein lineage markers and group in hematopoietic lineages

To establish a correlation between cell clusters identified in scRNAseq (11 clusters) and CyTOF (23 clusters), patterns of protein markers and their corresponding coding genes were correlated. Protein/gene combinations were tested on three different marker panels: (**a**) The B-cell markers *Itgam* (CD11b), *Cd19* (CD19), *Spn* (CD43), *Ptprc* (B220), *Kit* (CD117), *H2-Ab1* (MHC-II), (**b**) the T-cell markers *Cd5* (CD5), *Cd4* (CD4), *Cd8a* (CD8a), *Cd8b1* (CD8b), *Il2ra* (CD25), *Spn* (CD43), *Izumo1r* (FR4), and (**c**) the myeloid cell markers *Itgam*

(CD11b), *Itgax* (CD11c), *Ly6c1* (Ly-6C), *Ly6g* (Ly-6G), *Fcer1g* (CD64), and *Adgre1* (F4/80). Correlations were calculated with a Pearson coefficient (-1 to +1) and displayed in a correlation matrix after hierarchical column and row clustering. Dendrograms shown underneath each correlations matrix correspond to rows and columns.

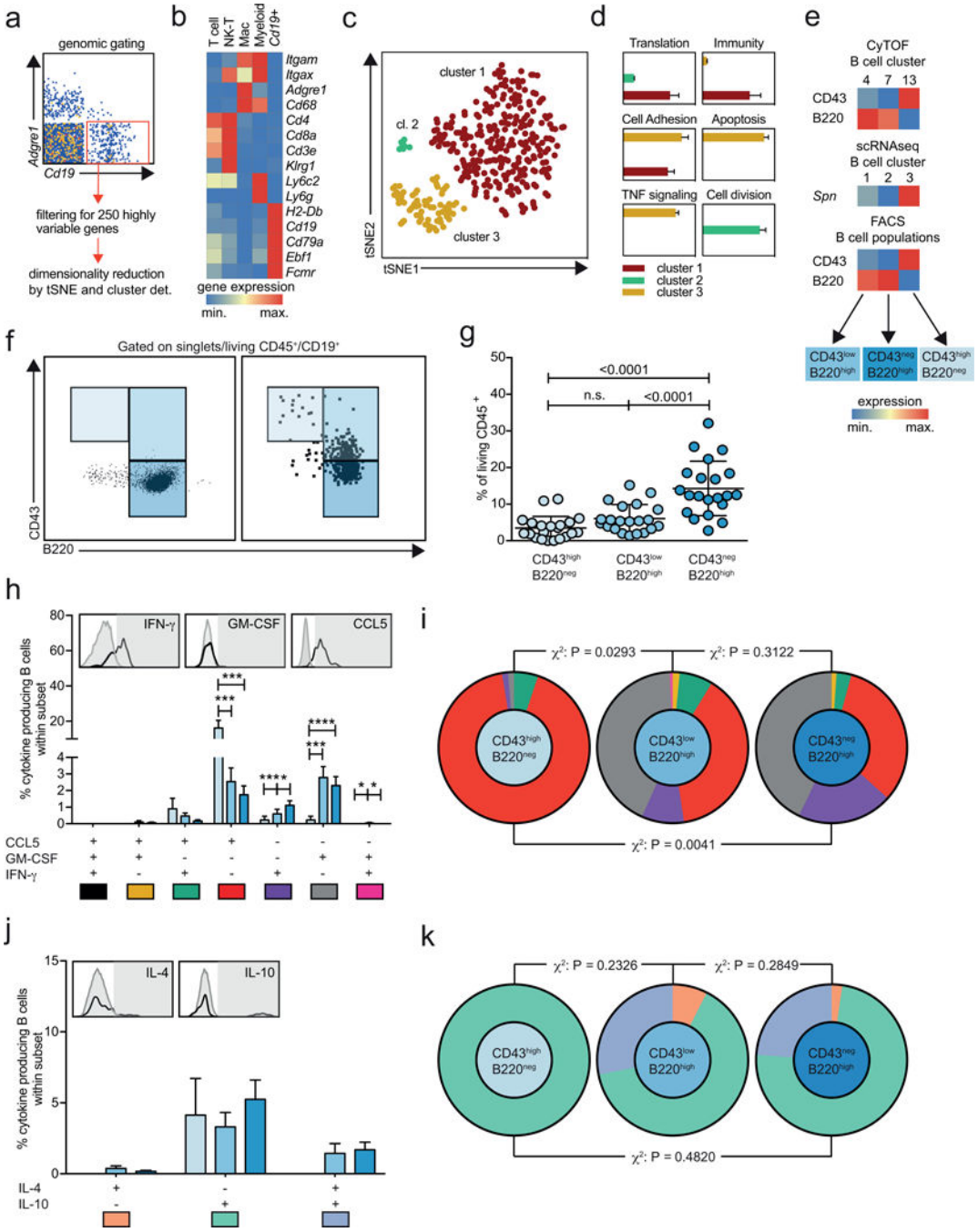

Figure 6. Transcriptional, phenotypic, and functional profiles identify three principal aortic B-cell sub-populations

(**a**) *Cd19*$^{+}$ *Adgre1*^{neg} single cell transcriptomes from aortic leukocytes from 10-pooled *Apoe*$^{-/-}$ mice after 12 weeks of WD were filtered in SeqGeq and (**b**) further analyzed for gene expression coding for lineage-defining leukocyte markers. Expression values were normalized in row scores for leukocyte clusters (T-cells, Nk-cells, macrophages, *Adgre1*^{neg} myeloid cells) and *Cd19*$^{+}$ *Adgre1*^{neg} events. (**c**) tSNE map and K-means clustering after dimensionality reduction of the top 250 highly variable genes. (**d**) The three retrieved

clusters were analyzed for differentially expressed genes and the significantly (P<0.05, FDR<0.05) upregulated genes served as input for pathway analysis. Pathways were grouped in functional classes and the enrichment score was plotted on the x-axis. (**e**) Gene and protein expression of the B cell surface markers CD43 (gene *Spn*) and B220 in the three principal B cell subsets independently identified in CyTOF (upper), scRNAseq (middle), and flow cytometry (FACS, lower heatmap). (**f**) Gating strategy to separate aortic B-cells (left) from *Apoe*$^{-/-}$ mice fed a WD for 12 weeks (n=21) based on CD43 and B220 expression. Fluorescence minus one (FMO) control is shown on the right. (**g**) Fraction of CD43^{high}B220^{neg}, CD43^{neg}B220^{high}, and CD43^{low}B220^{high} B cells among all aortic leukocytes. (**h,j**) Fraction of cells expressing different combinations of cytokines among the three B-cell sub-sets after stimulation with PMA/ionomycin for 5 hours. (**i,k**) The cytokine expression profiles of the three aortic B-cell populations was compared by a χ^2 test. (**g,h,j**) Statistical significance was calculated by a one-way ANOVA. Data are presented as mean ±SEM. *P<0.05, **P<0.01, ***P<0.001.

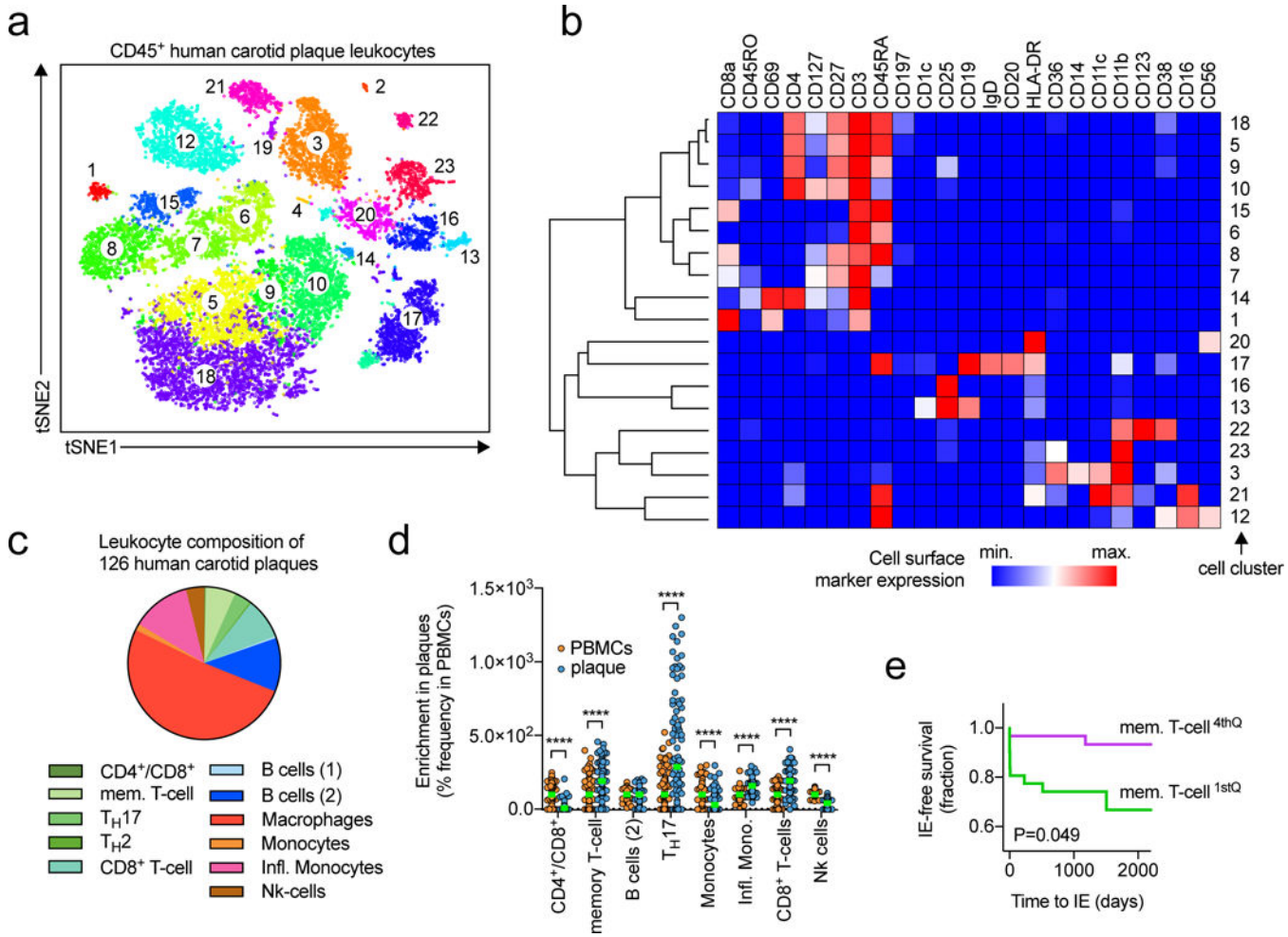

Figure 7. The frequency of aortic leukocyte populations predicts clinical events in patients with atherosclerosis

(**a**) Unsupervised cell cluster detection by a modified tSNE and CyTOF cluster detection algorithm (PhenoGraph) on CD45$^+$, live, DNA$^+$ leukocytes from human carotid plaques after endarterectomy and staining with an anti-human antibody panel and acquisition in CyTOF (full panel in Online-TableVIII). (**b**) Median expression of surface markers per clusters shown in a hierarchically clustered heatmap (row and column). A cluster frequency of >1% CD45$^+$, live, DNA$^+$ events was applied. The heatmap was normalized across clusters. (**c**) Genetic deconvolution of leukocyte cluster gene signatures in a set of bulk mRNA expression of 126 human carotid plaques from the BIKE-biobank to enumerate the relative abundance of cell clusters. The relative frequency of the tested clusters is shown. (**d**) Relative enrichment of leukocyte populations in plaques vs. PBMCs displayed as % of the frequency within PBMCs. (**e**) Kaplan-Maier survival curve of the ischemic event (IE) free survival after thrombendarterectomy. Myocardial infarction and stroke were classified as cardiovascular events. The frequency of memory T-cells was separated into quartiles and the lowest (1st) and highest (4th) were compared. Data are presented as mean±SEM. Significance was determined by a two-sided, unpaired Students T-test (**d**) or ANOVA (**c**). ****P<0.0001 or a Logrank and Gehan-Breslow-Wilcoxon test for survival curves (**e**). 126

individual human plaques were included in (**c**), N>97 per group (**d**). Number of IEs were 9 (1^{st}) and 2 (4^{th}) (**e**).